-SUPPORTING INFORMATION-

for

Stimulated X-ray Raman Imaging of Conical Intersections

Daeheum Cho* and Shaul Mukamel*

Department of Chemistry and Physics and Astronomy, University of California, Irvine, California 92697-2025, USA

E-mail: daeheumc@uci.edu; smukamel@uci.edu

Computational Details for the Surface Hopping Nonadiabatic Dynamics Simulations

The surface hopping simulation protocol implemented in SHARC[1,2] program was employed to simulate the nonadiabatic photodissociation of thiophenol. Details of the protocol are given in ref.[2] The electronic structure calculations were performed using MOLPRO[3] program at the state-averaged CASSCF(4/6)/6-31G* level of theory with four lowest adiabatic electronic states are taken into account. The local diabatization algorithm based on the overlap matrices between the adiabatic electronic states $\langle\psi_\beta(t)|\psi_\alpha(t+\Delta t)\rangle$ is used to propagate the electronic wavefunction under the effect of nonadiabatic couplings, while the nuclear coordinates are propagated using Newtons equations. Surface hopping probability is calculated as described in ref.[2] Given the coefficient vectors $\boldsymbol{c}(t)$ and $\boldsymbol{c}(t+\Delta t)$ and the corresponding propagator matrix $\boldsymbol{P}$, hopping probabilities from electronic state β to α is calculated by

$$h_{\beta\to\alpha} = \left(1 - \frac{|c_\beta(t+\Delta t)|^2}{|c_\beta(t)|^2}\right) \frac{\Re\left[c_\alpha(t+\Delta t)(P_{\alpha\beta})^*(c_\beta(t))^*\right]}{|c_\beta(t)|^2 - \Re\left[c_\beta(t+\Delta t)(P_{\beta\beta})^*(c_\beta(t))^*\right]}. \tag{S1}$$

We employed the energy-based decoherence correction scheme to describe the electronic decoherence when two surfaces drift away after passing the CI.[4] In this decoherence scheme, the wavefunction coefficients are rescaled according to the relation below.

$$c'_\alpha = c_\alpha \cdot \exp\left[-\Delta t \frac{|E_\alpha - E_\beta|}{\hbar}\left(1 + \frac{C}{E_{\text{kin}}}\right)^{-1}\right], (\alpha \neq \beta), \tag{S2}$$

$$c'_\beta = \frac{c_\beta}{|c_\beta|} \cdot \left[1 - \sum_{\alpha\neq\beta} |c'_\alpha|^2\right] \tag{S3}$$

The electronic population (ρ_{ii}; diagonal element of the density matrix) and the coherence (ρ_{ij}; off-diagonal element of the density matrix) in the adiabatic electronic state can be calculated from the wavefunction coefficient vector $\boldsymbol{c}(t)$, $\rho_{ii}(t) = |c_i(t)|^2$ and $\rho_{ij}(t) = c_i(t)c_j^*(t)$. The

Raman shift $|\Delta E_{ij}|$ was obtained from the energy difference between the adiabatic electronic states S_i and S_j. The transition charge density $\sigma_{ij}(\boldsymbol{r})$ is calculated at every nuclear time step to account the geometrical change. All quantities presented in the paper are in the adiabatic electronic basis. The total propagation time was 49 fs and the time steps for propagation of the nuclear and the electronic degrees of freedom were 0.05 fs and 0.002 fs, respectively. 45 initial geometries were sampled by using the quantum harmonic oscillator Wigner distribution at around the ground state equilibrium geometry. The nonadiabatic surface hopping dynamics was initiated by promoting the system on S_2 ($^1\pi\sigma^*$) state. 45 trajectories were simulated and averaged out to provide the signals. Fig. S2-4 shows the convergence of the population dynamics ρ_{ii} and coherences ρ_{12} and ρ_{01} with the number of trajectories taken into account.

We have investigated the dynamics of the S-H dissociation of thiophenol that takes place after its initial photoexcitation in S_2 ($^1\pi\sigma^*$) state (impulsive excitation approximation; no external pump pulse was taken into account in the surface hopping dynamics). In practice, excitation at long wavelength $\lambda > 275$ nm excites the system to $1^1\pi\pi^*$ state, while the $^1\pi\sigma^*$ state can be excited at shorter excitation wavelengths.[5–7] H-tunnelling from $1^1\pi\pi^*$ state to $^1\pi\sigma^*$ state may play a role in the photodissociation of thiophenol after an excitation to S_1 ($1^1\pi\pi^*$) state, which may not be properly described by the semi-classical surface hopping method. It is known that H-tunnelling plays an important role in a photodissociation of phenol after excitation to S_1 ($1^1\pi\pi^*$) state.[8–10] Therefore, a photodissociation dynamics following an initial excitation to S_2 ($^1\pi\sigma^*$) state was considered in this paper.

The electronic population and the coherence can be calculated from the wavefunction coefficient vector $\boldsymbol{c}(t)$, $\rho_{ii}(t) = |c_i(t)|^2$ and $\rho_{ij}(t) = c_i(t)c_j^*(t)$. Raman shift $|\Delta E_{ij}|$ was obtained from the energy difference between the electronic states. We employed the energy-based decoherence correction scheme to describe the electronic decoherence when two surfaces drift away after passing the CI.

The Signal

The SXRI signal is defined as the time-integrated rate of change of photon number in the (attosecond) broadband field $\boldsymbol{A}_1$

$$S(\omega, \mathbf{k}_s) = \int d\boldsymbol{r}dt\langle\frac{d}{dt}\hat{N}^1_\omega\rangle = \int d\boldsymbol{r}dt\langle\frac{d}{dt}\hat{\boldsymbol{A}}^\dagger_1 \cdot \hat{\boldsymbol{A}}_1\rangle \tag{S4}$$

where the $\hat{N}^1_\omega$ is the number operator for the photon mode with frequency ω and the 1 superscript indicates restriction to modes occupied by the $\hat{\boldsymbol{A}}_1$.

Using the Heisenberg equation of motion for the operator with the minimal-coupling interaction Hamiltonian in the off-resonant limit, by discarding the resonant interaction term $\hat{\boldsymbol{j}} \cdot \hat{\boldsymbol{A}}$, is given by,

$$H_{\text{int}}(t) = \frac{1}{2}\int d\boldsymbol{r}\left(\hat{\sigma}(\hat{\boldsymbol{A}}^\dagger_0\hat{\boldsymbol{A}}_1 + \hat{\boldsymbol{A}}^\dagger_0\hat{\boldsymbol{A}}_1)\right) \tag{S5}$$

where $\hat{\sigma}$ is the charge density operator and the vector potential is expressed as the field mode expansion

$$\hat{\boldsymbol{A}}(\boldsymbol{r}) = \sum_{\boldsymbol{k}_j\lambda_j}\sqrt{\frac{2\pi}{\Omega\omega_j}}\left(\epsilon^{(\lambda_j)}(\boldsymbol{k}_j)\hat{a}_j e^{i\mathbf{k}_j\cdot\boldsymbol{r}} + \epsilon^{(\lambda_j)*}(\boldsymbol{k}_j)\hat{a}^\dagger_j e^{-i\mathbf{k}_j\cdot\boldsymbol{r}}\right) \tag{S6}$$

where $\hat{a}_j$ ($\hat{a}^\dagger_j$) the photon field boson annihilation (creation) operator for mode j, Ω the field quantization volume, and $\epsilon^{(\lambda_j)}(\mathbf{k}_j)$ the polarization vector.

We start with the Heisenberg equation of motion for the photon number operator $\hat{N}^1_\omega = \hat{\boldsymbol{A}}^\dagger_1\hat{A}_1$

$$\langle\frac{d}{dt}(\hat{\boldsymbol{A}}^\dagger_1 \cdot \hat{\boldsymbol{A}}_1)\rangle = \langle\frac{d}{dt}(\hat{\boldsymbol{A}}^\dagger_1) \cdot \hat{\boldsymbol{A}}_1\rangle + c.c. = 2\Re\langle\frac{d}{dt}(\hat{\boldsymbol{A}}^\dagger_1) \cdot \hat{\boldsymbol{A}}_1)\rangle. \tag{S7}$$

The time derivative in the last term can be calculated

$$\frac{d}{dt}\hat{\boldsymbol{A}}_1^\dagger = -i[\hat{H}_{\text{int}}, \hat{\boldsymbol{A}}_1^\dagger] = -\frac{i}{2}\int d\boldsymbol{r}'[\hat{\sigma}(\hat{\boldsymbol{A}}_0^\dagger\hat{\boldsymbol{A}}_1 + \hat{\boldsymbol{A}}_0^\dagger\hat{\boldsymbol{A}}_1), \hat{\boldsymbol{A}}_1^\dagger] = -\frac{i}{2}\int d\boldsymbol{r}'[\hat{\sigma}(\hat{\boldsymbol{A}}_0^\dagger\hat{\boldsymbol{A}}_1 + \hat{\boldsymbol{A}}_0\hat{\boldsymbol{A}}_1^\dagger), \hat{\boldsymbol{A}}_1^\dagger] \tag{S8}$$

$$= -\frac{i}{2}\int d\boldsymbol{r}'[\hat{\sigma}\hat{\boldsymbol{A}}_0^\dagger\hat{\boldsymbol{A}}_1, \hat{\boldsymbol{A}}_1^\dagger] = -\frac{i}{2}\int d\boldsymbol{r}'\hat{\sigma}\hat{\boldsymbol{A}}_0^\dagger \tag{S9}$$

where we have used $[\hat{\boldsymbol{A}}_1, \hat{\boldsymbol{A}}_1^\dagger] = 1$, $[\hat{\boldsymbol{A}}_0^\dagger, \hat{\boldsymbol{A}}_1^\dagger] = 0$, $[\hat{\boldsymbol{A}}_0\hat{\boldsymbol{A}}_1^\dagger, \hat{\boldsymbol{A}}_1^\dagger] = 0$, $[\hat{\boldsymbol{A}}_0\hat{\boldsymbol{A}}_1^\dagger, \hat{\boldsymbol{A}}_1^\dagger] = 0$, and $[\hat{\boldsymbol{A}}_0^\dagger\hat{\boldsymbol{A}}_1, \hat{\boldsymbol{A}}_1^\dagger] = \hat{\boldsymbol{A}}_0^\dagger$. Plugging eq. S9 into eq. S7, we have

$$S(\omega, \mathbf{k}_s) = \int d\boldsymbol{r}dt\langle\frac{d}{dt}\hat{\boldsymbol{A}}_1^\dagger \cdot \hat{\boldsymbol{A}}_1\rangle = 2\Re\int d\boldsymbol{r}dt\langle\frac{d}{dt}(\hat{\boldsymbol{A}}_1^\dagger) \cdot \hat{\boldsymbol{A}}_1)\rangle = -\Im\int d\boldsymbol{r}d\boldsymbol{r}'dt\langle\hat{\sigma}\hat{\boldsymbol{A}}_0^\dagger \cdot \hat{\boldsymbol{A}}_1\rangle \tag{S10}$$

$$= -\Im\int dtd\boldsymbol{r}d\boldsymbol{r}'e^{i\mathbf{k}_s(\boldsymbol{r}-\boldsymbol{r}')}\boldsymbol{\mathcal{A}}_0(\boldsymbol{r}', t)\boldsymbol{\mathcal{A}}_1^*(\boldsymbol{r}, t)\langle\hat{\sigma}(\boldsymbol{r}', t)\rangle. \tag{S11}$$

By assuming that the probe pulses have plane wave-like spatial variation

$$\boldsymbol{\mathcal{A}}_0(\boldsymbol{r}', t) = \boldsymbol{\mathcal{A}}_0(t)e^{i\mathbf{k}_0\cdot\boldsymbol{r}'} \tag{S12}$$

$$\boldsymbol{\mathcal{A}}_1(\boldsymbol{r}, t) = \boldsymbol{\mathcal{A}}_1(t)e^{i\mathbf{k}_1\cdot\boldsymbol{r}} \tag{S13}$$

and integrating over $\boldsymbol{r}$ and $\boldsymbol{r}'$,

$$S(\omega, \boldsymbol{q}, T) = -\Im\int dte^{i\omega(t-T)}\boldsymbol{\mathcal{A}}_1^*(\omega)\boldsymbol{\mathcal{A}}_0(t-T)\langle\hat{\sigma}(\boldsymbol{q}, t)\rangle \tag{S14}$$

where we have used

$$\langle\sigma(\boldsymbol{q}, t)\rangle = \int d\boldsymbol{r}e^{-i\boldsymbol{q}\cdot\boldsymbol{r}}\langle\sigma(\boldsymbol{r}, t)\rangle. \tag{S15}$$

When we expand the signal in the molecular eigenbasis,

$$S(\omega, \boldsymbol{q}, T) = \int \mathrm{d}te^{i\omega(t-T)}\boldsymbol{\mathcal{A}}_1^*(\omega)\boldsymbol{\mathcal{A}}_0(t-T)\sum_{a,c}\rho_{ac}(t)\sigma_{ac}(\boldsymbol{q}, t). \tag{S16}$$

The time-dependence of $\sigma(\boldsymbol{q}, t)$ arises from the nuclear dynamics.

Frequency-Resolved SXRI signal

Fig. S1 shows the simulated SXRI signal at different detection frequency ω. The SXRI signal appears when the electronic surfaces become close, i.e., at a small Raman transition frequency. Frequency-resolved SXRI signal reveals how the electronic transition between the surfaces occurs in the vicinity of conical intersections.

References

(1) Mai, S.; Marquetand, P.; Gonzlez, L. Nonadiabatic dynamics: The SHARC approach. *WIREs Comput Mol Sci* **2018**, *8*, e1370.

(2) Richter, M.; Marquetand, P.; Gonzlez-Vzquez, J.; Sola, I.; Gonzlez, L. SHARC: ab initio Molecular Dynamics with Surface Hopping in the Adiabatic Representation Including Arbitrary Couplings. *J. Chem. Theory Comput.* **2011**, *7*, 1253–1258.

(3) Werner, H.-J.; Knowles, P. J.; Knizia, G.; Manby, F. R.; Schtz, M. Molpro: a general-purpose quantum chemistry program package. *WIREs Comput Mol Sci* **2012**, *2*, 242–253.

(4) Granucci, G.; Persico, M.; Zoccante, A. Including quantum decoherence in surface hopping. *The Journal of Chemical Physics* **2010**, *133*, 134111.

(5) Lim, J. S.; Choi, H.; Lim, I. S.; Park, S. B.; Lee, Y. S.; Kim, S. K. Photodissociation Dynamics of Thiophenol- d_1 : The Nature of Excited Electronic States along the SD Bond Dissociation Coordinate. *J. Phys. Chem. A* **2009**, *113*, 10410–10416.

(6) Devine, A. L.; Nix, M. G. D.; Dixon, R. N.; Ashfold, M. N. R. Near-Ultraviolet Photodissociation of Thiophenol . *J. Phys. Chem. A* **2008**, *112*, 9563–9574.

(7) Venkatesan, T. S.; Ramesh, S. G.; Lan, Z.; Domcke, W. Theoretical analysis of photoinduced H-atom elimination in thiophenol. *The Journal of Chemical Physics* **2012**, *136*, 174312.

(8) Yang, K. R.; Xu, X.; Zheng, J.; Truhlar, D. G. Full-dimensional potentials and state couplings and multidimensional tunneling calculations for the photodissociation of phenol. *Chem. Sci.* **2014**, *5*, 4661–4680.

(9) Xu, X.; Zheng, J.; Yang, K. R.; Truhlar, D. G. Photodissociation Dynamics of Phenol: Multistate Trajectory Simulations including Tunneling. *J. Am. Chem. Soc.* **2014**, *136*, 16378–16386.

(10) Xie, C.; Ma, J.; Zhu, X.; Yarkony, D. R.; Xie, D.; Guo, H. Nonadiabatic Tunneling in Photodissociation of Phenol. *J. Am. Chem. Soc.* **2016**, *138*, 7828–7831.

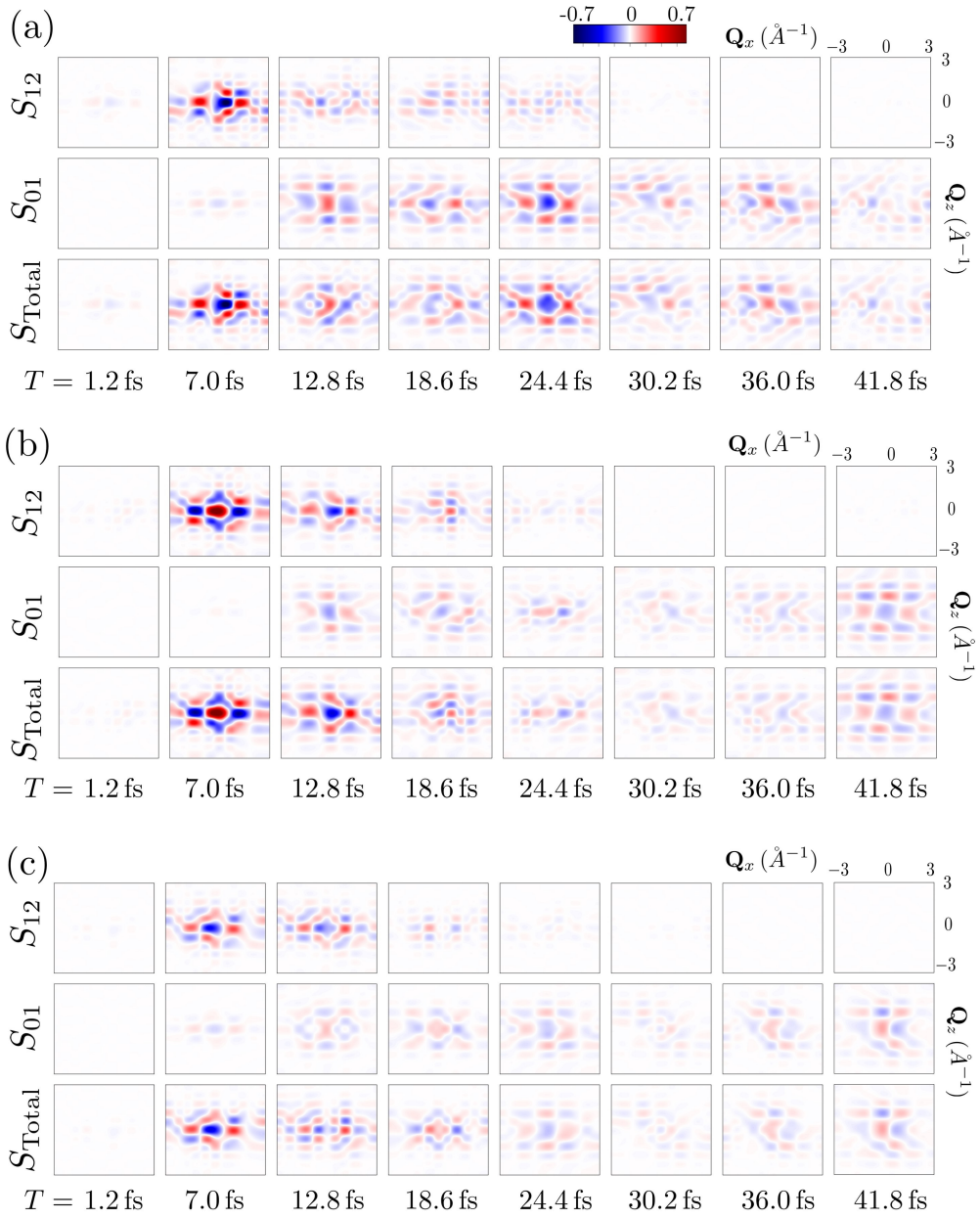

Figure S1: Simulated SXRI signal $S(\omega, \boldsymbol{Q}, T)$ for (a) $\omega = 0.5\,\text{eV}$, (b) $\omega = 1.5\,\text{eV}$, and (c) $\omega = -0.5\,\text{eV}$ at several time-delay T. S_{12} (S_{01}) represent the signal contribution from the $|1\rangle\langle 2|$ ($|0\rangle\langle 1|$) coherence, which is turned-on while passing through the CI-1 (CI-2). $S_{\text{Total}} = S_{01} + S_{12}$.

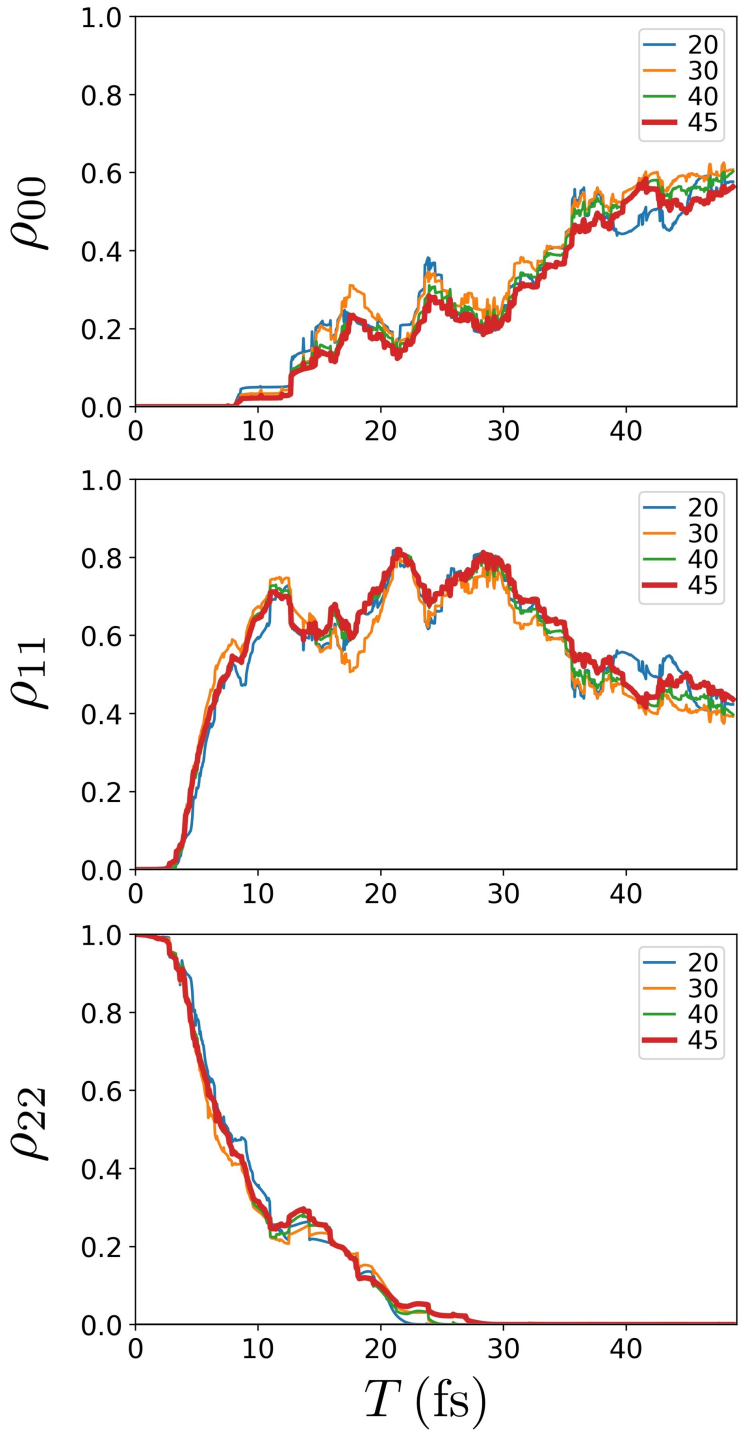

Figure S2: Convergence of the population dynamics ρ_{ii} for S_i state with the number of trajectories.

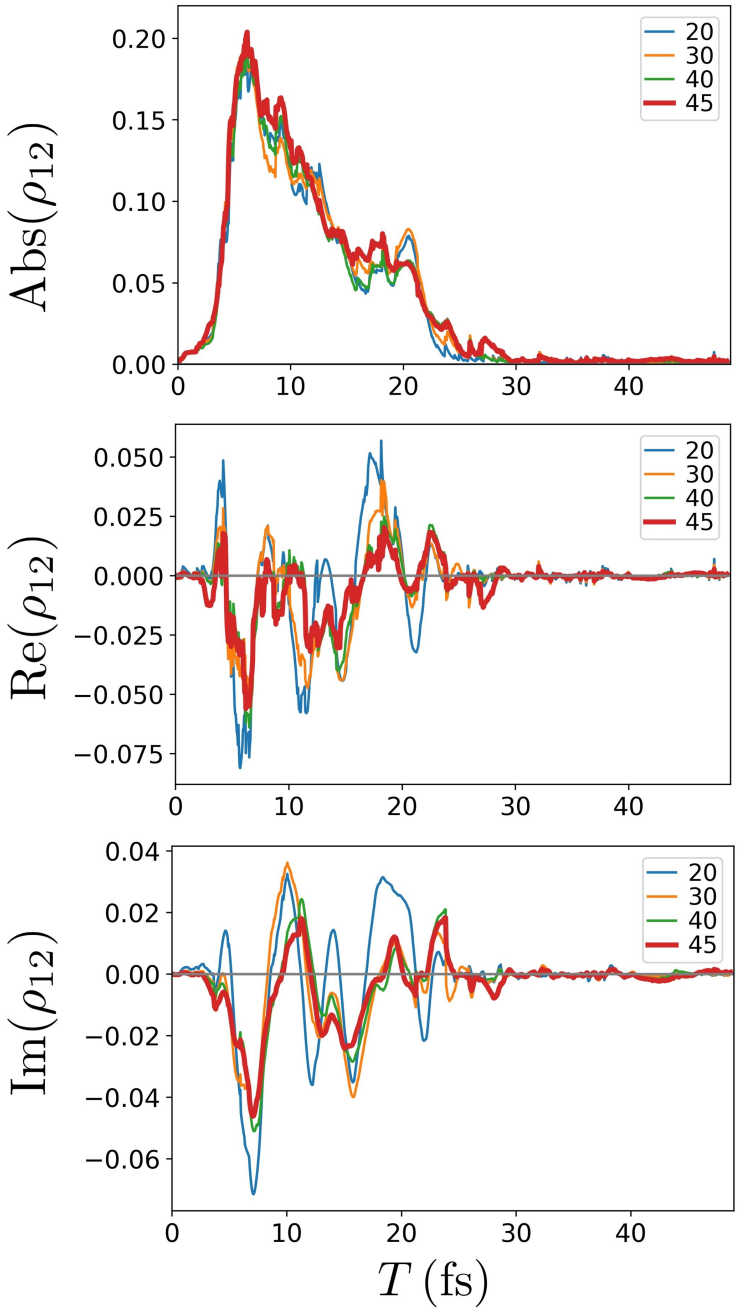

Figure S3: Convergence of the absolute, real, and imaginary values of the coherence $\rho_{12}(T)$ with the number of trajectories..

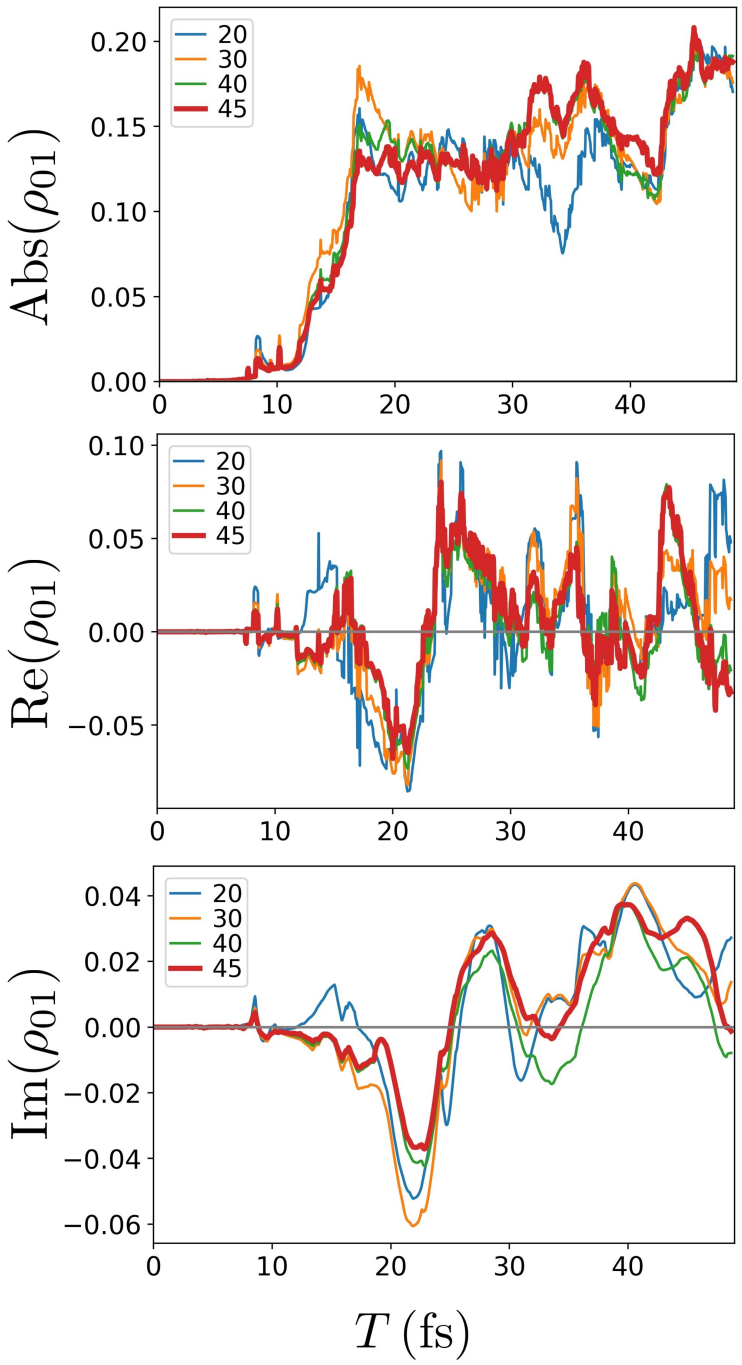

Figure S4: Convergence of the absolute, real, and imaginary values of the coherence $\rho_{01}(T)$ with the number of trajectories.